Article

Enhanced Signal Amplification in a TLR-4 Biosensor Utilizing Ferrocene-Terminated Mixed Monolayers

Robert M Mayall, Margaret Renaud-Young, Erin Gawron, Samantha Luong, Stephen E. Creager, and Viola I. Birss

ACS Sens., **Just Accepted Manuscript** • DOI: 10.1021/acssensors.8b01069 • Publication Date (Web): 18 Dec 2018

Enhanced Signal Amplification in a TLR-4 Biosensor Utilizing Ferrocene-Terminated Mixed Monolayers

Robert M. Mayall[1], Margaret Renaud-Young[1], Erin Gawron[1], Samantha Luong[1], Stephen Creager[2], and Viola I. Birss[1,].*

1 - Department of Chemistry, University of Calgary, Alberta, Canada.
2 - Department of Chemistry, Clemson University, Clemson, South Carolina, USA.

* - Corresponding author: birss@ucalgary.ca

Abstract

A major challenge in effectively treating infections is to provide timely diagnosis of a bacterial or viral agent. Current cell culture methods require >24 hours to identify the cause of infection. The Toll-Like Receptor (TLR) family of proteins can identify classes of pathogens and has been shown to work well in an impedance-based biosensor, where the protein is attached to an electrode via a self-assembled monolayer (SAM). While the sensitivity of these sensors has been good, they contain a high resistance (>1 kΩ) SAM, generating relatively small signals and requiring longer data collection, which is ill-suited to implementation outside of a laboratory. Here, we describe a novel approach to increase the signal magnitude and decrease the measurement time of a TLR-4 biosensor by inserting a redox-active ferrocenyl-terminated alkane thiol into a mixed SAM containing hydroxyl- and carboxyl-terminated alkane thiols. The SAM formation and modification was confirmed via contact angle and X-ray photoelectron spectroscopy measurements, with TLR-4 immobilization demonstrated through a modified immunosorbent assay. It is shown that these TLR-4 biosensors respond selectively to their intended target, Gram-negative bacteria at levels between 10^0 and 10^5 lysed cells/mL, while remaining insensitive to Gram-positive bacteria or viral particles at up to 10^5 particles/mL. Furthermore, the signal enhancement due to the addition of ferrocene decreased the measurement time to less than one minute and has enabled this sensor to be used with an inexpensive, portable, handheld potentiostat that could be easily implemented in field settings.

Keywords: Mixed self-assembled monolayers, Toll-Like Receptor biosensor, TLR-4, Gram-negative bacteria, ferrocene.

Table of Contents Graphic:

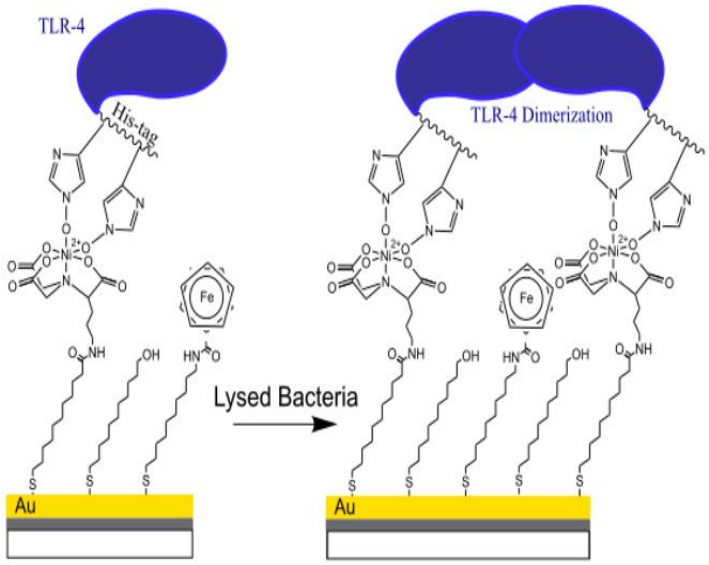

The rapid and accurate detection and classification of bacteria is of great concern for both medical and security applications. However, the standard detection method for bacterial identification is to culture the cells in a laboratory.[1] This process is slow and laborious, often taking multiple days before the presence of bacteria in a sample is confirmed. This delay between presentation and detection is detrimental to patients who could go untreated or to potential victims of biological warfare due to failure to detect and quarantine a pathogen.[1] As such, there is a need for the development of a rapid and sensitive detection system capable of determining the presence of bacteria beyond the setting of a diagnostic laboratory.

In recent years, biosensor technology has shown excellent promise in addressing this need, with many publications focussed on the use of polymerase chain reactions and antibody-based sensors.[2,3] While these systems (and others) have shown good detection thresholds, the use of specific probe sequences or antibodies requires an understanding of the specific target. Unbiased testing for biological agents would require thousands of sensors for all possible permutations of potential pathogens. Thus, there is a need for a sensor that can detect the presence of a biological agent without prior knowledge of what the specific agent may contain.

In the human body, this pathogen classification is performed by the innate immune system, which recognizes highly conserved biomolecules of bacterial and viral origin, known as pathogen-associated molecular patterns.[4] The family of Toll-like Receptor proteins are pattern recognition receptors of the innate immune system that form dimers upon binding their targets, initiating signals in the immune cells that facilitate the appropriate immune response. Toll-Like Receptor-4 (TLR-4) responds selectively to lipopolysaccharide (LPS), a molecule that is present only in Gram-negative bacterial cell walls.[5] The use of TLR-4 proteins in a sensor would thus

greatly facilitate the diagnosis of pathogens and the treatment of an infection, as Gram-negative and Gram-positive bacteria can be treated with different antibiotics.[6]

A number of published papers have demonstrated that TLR-4 and the other proteins in the Toll-Like Receptor family can be utilized in biosensors that are based on spectroscopy or electrochemistry, showing significant promise in being able to differentiate classes of bacteria and other biological threat agents.[7–12] This is especially true for the use of TLR-based impedance sensors, where the protein is attached to an electrode via a linker, such as a self-assembled monolayer (SAM).[7,8,11,13–15] However, some of these impedance-based sensors have tended to require measurement times of ≥10 min, which is distinct from an incubation period of typically 30 minutes that is needed to allow the TLR to interact with the target molecule, while also generating relatively small signals due to their high resistances (>1 kΩ).[7,8,13,15,16] The high sensor resistance would thus necessitate the use of research-grade instrumentation, making them ill-suited to implementation outside of a laboratory.

In our previous work, TLR-4 was tethered to a Ni^{2+}-nitrilotriacetic acid (NTA) functional group that was covalently attached to the end of a carboxyl-terminated undecanethiol-based self-assembled monolayer (SAM) on a Au surface. The receptor was oriented in a bio-mimicking fashion such that, when TLR-4 dimerizes in the presence of LPS, the access of a soluble redox probe, e.g., $Fe^{2+/3+}$, to the underlying Au is restricted.[7] As well, attempts were made to lower the resistance of the TLR-4/SAM/Au electrode/solution interface by attaching short spacer thiols (1-propanethiol) between the 11-mercaptoundecanoic acid thiols, which were modified to bind to TLR-4. The sensor was then able to detect trace levels of Gram-negative bacteria and purified LPS while remaining completely insensitive to Gram-positive bacteria or viral particles. However, this mixed SAM was still quite resistive (ca. 10^6 Ω), resulting in a large time constant

and small currents. There is also evidence in the literature that mixed SAMs composed of thiols with vastly different chain lengths do not form stable monolayers.[17,18]

Sensor Design Strategy

To address these deficiencies, this work focused on lowering the resistance of a TLR-4 biosensor through the use of mixed thiol SAMs with different terminal functional groups, as in our previous design,[7] but now with similar length alkyl backbone chains. As stated above, a common disadvantage of long alkyl chain SAMs is that the resistance of the surface film can be quite large, producing small signals to detect the subtle changes introduced by the TLR-4/LPS interactions, especially in field-deployable devices. This high resistance arises from the very low rate constant for heterogeneous electron transfer between redox species in solution and the underlying electrode, caused by the long distance and weak electronic coupling between the SAM and the redox species. To circumvent this problem and achieve larger signals, we have inserted a small quantity of ferrocenyl-terminated thiol in the mixed SAMs to serve as redox active sites (Scheme 1). This allows for the use of these long-chain thiols that have been previously shown to increase the stability of the monolayer compared to shorter-chain thiols,[19–21] with 11-mercaptoundecanoic acid (carboxyl-terminated), 11-mercaptoundecanol (hydroxyl-terminated) and 10-mercaptodecyl-ferrocenylcarboxamide (ferrocenyl-terminated) chosen for this work (Scheme 1).

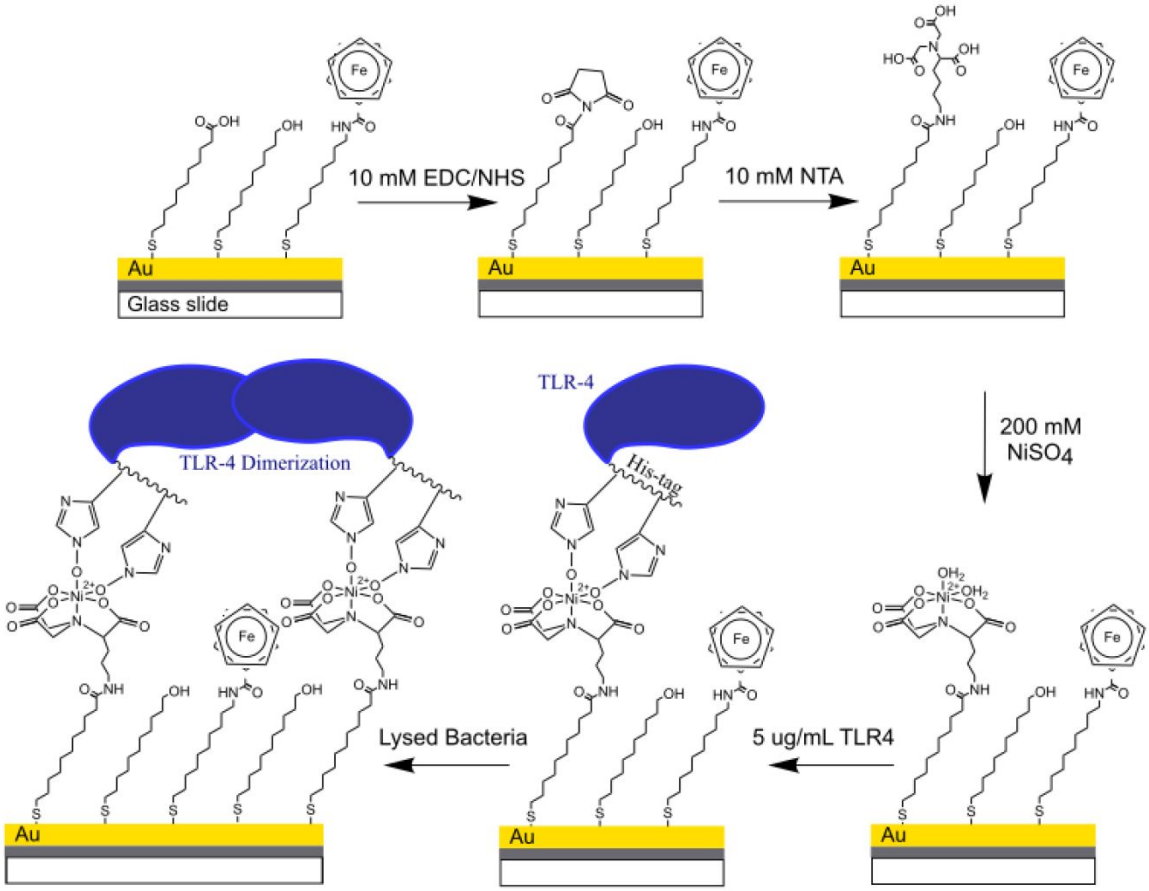

Scheme 1. Schematic representation of the proposed SAM design containing ferrocenyl-terminated thiols mixed with similar chain length carboxylic acid and hydroxyl terminated thiols. Carboxylic acid terminated thiols form amide bonds to nitrilotriacetic acid (NTA) functional group and then chelate Ni^{2+} to immobilize TLR-4 through interactions with a poly-histidine tag. When TLR-4 is exposed to lipopolysaccharide (LPS) from lysed Gram-negative bacteria, it dimerizes and blocks access of ferrocyanide in solution to ferrocenyl-terminated thiols, thus increasing resistance of Fe(II)/(III) reaction.

As previous literature has shown, when a ferrocene group in a SAM is oxidized to ferricenium in the presence of ferrocyanide, an electrochemical mediation event occurs.[22] This is based on the oxidation of ferrocyanide to ferricyanide by ferrocene, while it prevents reduction back to ferrocyanide, due to the mismatch of the relative $E^{0'}$ values for the ferrocene/ferricenium couple (ca. 0.40 V vs Ag/AgCl) and the ferro/ferricyanide couple (ca. 0.25 V vs Ag/AgCl). This results in much larger anodic currents than seen for either a comparable ferrocene SAM or for the oxidation of ferrocyanide at a similar non-ferrocenyl-terminated SAM, and quite small

cathodic currents, often referred to as rectification.[22–24] This strategy for the generation of signals in an electrochemical biosensor has been previously explored, e.g., in the design of DNA-based biosensors.[25–28]

In the present work, the SAMs were not constructed solely from either ferrocenyl-terminated or carboxyl-terminated thiols, as these have been shown to form relatively unstable monolayers.[29,30] Instead, a tripartite SAM was constructed by placing inert hydroxyl-terminated "spacer" thiols between the carboxyl and redox-active ferrocenyl-terminated thiols (Scheme 1).[22,31–33] An additional benefit of the hydroxyl-terminated thiols is their reported ability to create interfaces with a resistance towards fouling by nonspecific adhesion, which could be beneficial to the future implementation of the results of this work in field samples.[34] The thiols used to form the SAM in the present work were of similar length (Scheme 1), as alkanethiols of similar lengths have been shown to mix more thoroughly and form stable SAMs.[35]

Previous work demonstrated that ferrocenyl-terminated thiols comprising 5-10% of the total SAM composition produces reproducible voltammograms (indicative of facile electron transfer across the SAM) and rectification in the presence of ferrocyanide in solution.[22] For this reason, a 5% concentration of ferrocenyl-terminated thiol was mixed with carboxylate- and hydroxyl-terminated thiols in the present sensor design. As in our previous work, the carboxyl-terminated thiols were modified to form an amide bond to a nitrilotriacetic acid-containing moiety that could subsequently chelate a Ni^{2+} cation and then immobilize the histidine-tagged TLR-4 protein.[7]

It is shown here, for the first time, that a sensor based on a mixed SAM, composed of carboxyl-, ferrocenyl- and hydroxyl-terminated thiols, produces a highly sensitive TLR-4-based sensor with a significantly lowered resistance compared to sensors without the ferrocene group.

The ferrocene-based sensor does not respond to the presence of Gram-positive bacteria or viral particles, with all tested sensors having a low (≤1 kΩ) resistance in the ferrocyanide solution. Compared to state-of-the-art TLR-based biosensors,[7,9,13] the sensors described here provide both a marked decrease in resistance and a significantly shorter measurement time for LPS detection. This ferrocene-SAM based sensor can also operate with an inexpensive (<$100), open-source potentiostat, a key benefit for any application outside of a laboratory. The attachment of a redox-active group in the SAM to increase the analyte signal could be applied to any electrochemical sensor in which the current depends on restricting the access of a soluble redox species to the underlying electrode surface.

Materials & Methods

The Au electrodes were rinsed sequentially with ethanol and water before being electrochemically cleaned in 0.5 M H_2SO_4 between 0.05 V and 1.7 V vs RHE at 500 mV/s until the cyclic voltammograms obtained no longer changed.[7,36] The electrodes were then submerged for 24 hours in 1 mM thiol solution containing the desired thiol mixture, assuming that 5% MFc in solution would correspond to 5% MFc on the Au surface. The Au/SAM electrodes were then placed in a mixture of 0.108 g 2-(N-morpholino)ethanesulfonic acid with 5.5 mg N-hydroxysuccinimide and 2 mg 1-ethyl-3-(3-dimethylaminopropyl)carbodiimide hydrochloride in 5 mL of ultrapure water for one hour under nitrogen gas.[7,37]

The electrodes were then transferred to 1 mM bis(carboxymethyl)-L-lysine in order to covalently attach a nitrilotriacetic acid (NTA) functional group to the distal end of the 11-mercaptoundecanoic acid thiols in the SAM at 4 °C overnight. The electrodes were then soaked for 20 minutes in 0.1 M $NiSO_4$ to form the Ni^{2+}-NTA modified surface before 20 minutes of

exposure to TLR-4/MD-2, reconstituted in 0.2 M pH 7 phosphate buffer (to ensure protein stability) to a concentration of 5 μg/mL.

Gram-negative (heat killed *Salmonella typhimurium*), Gram-positive (heat killed *Staphylococcus aureus*) or viral (UV-inactivated *Rahbdovirus*) challenges were added sequentially from stock solutions of 10^{10} particles/mL in pH 7 0.2 M phosphate buffer after a baseline measurement was performed. Baselines were always measured and used to normalize the data, as SAM formation is somewhat stochastic in nature and the exact content of the ferrocene thiol in the SAM could not be precisely duplicated (experimental coverages ranged from 5-10 x 10^{12} molecules/cm^2). The solutions were then mixed thoroughly with a micropipette, followed by an additional 20 minutes of deaeration and mixing by bubbling with nitrogen and retesting in order to determine if the sensor responded to the challenge.

Results and Discussion

TLR-4 Sensor Construction and Verification

Preliminary experiments were performed first with just the ferrocene-based SAMs (Scheme 1a) to determine the coverage of the ferrocene thiol and whether the ferrocenyl-terminated thiol in the SAM would produce the expected signal amplification (through a mediation reaction).[22] The electrochemical response of a tripartite SAM, containing 30% 11-mercaptoundecanoic acid (MUA, carboxylic acid), 65% 11-mercaptoundecanol (MUO, hydroxyl), and 5% 10-mercaptodecyl-ferrocenylcarboxamide (MFc, ferrocene) thiols, was thus obtained in 0.2 M PBS. As in prior literature,[21,38] it was assumed that the composition of the SAMs formed on Au from a solution containing a mixture of thiols would be similar to the composition of the thiol-containing solution.

As seen in Fig 1a (solid black line), the oxidation/reduction of the ferrocene thiol within the mixed SAM is clearly visible in the form of a surface-confined set of peaks, as reported previously.[22,23,39] The anodic (and cathodic, not shown) peak currents trend linearly with sweep rate (Figure 1b), indicating that the ferrocene group is surface-confined, while the near zero peak separation, for all scan rates tested, indicates rapid electron transfer kinetics for the surface-bound ferrocene species. The surface coverage of the ferrocene component in Fig 1a was determined to be ca. 7.4 x 10^{12} molecules/cm^2, although coverages ranged from 5-10 x 10^{12} molecules/cm^2 between replicates. The coverage was determined by integrating the CV charge passed during ferrocene oxidation and normalizing to the real Au surface area, determined from the Au oxide reduction charge (after electrochemical cleaning) of 390 μC/cm^2 after scanning to 1.7 V vs. RHE.[40]

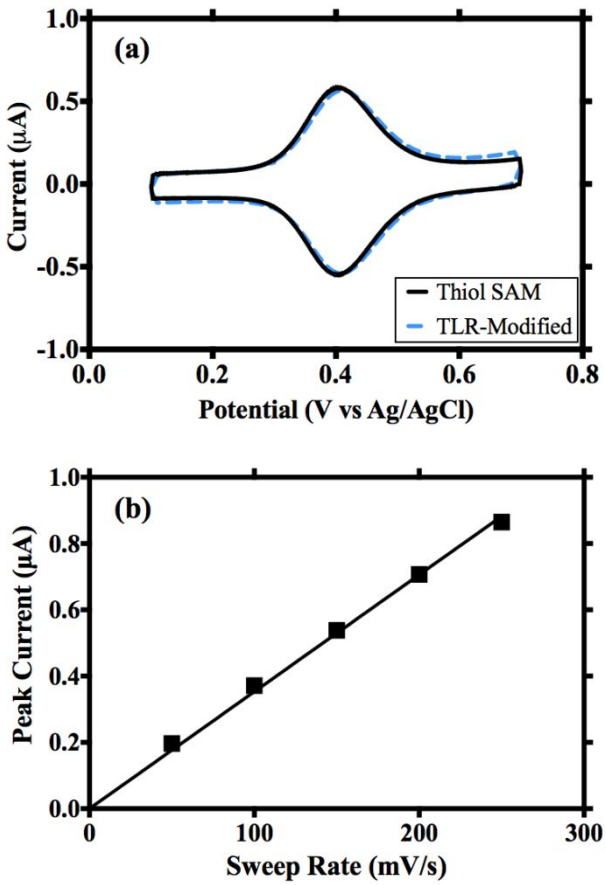

Figure 1. (a) CV (100 mV/s) of 30%MUA/5%MFc/65%MUO SAM on Au before (solid black line) and after (dashed blue line) derivatization and immobilization of TLR-4. **(b)** Relationship between peak current and scan rate for the TLR-4 modified SAM. CVs were performed in 0.2 M pH 7 phosphate buffer + 5 mM $K_4Fe(CN)_6$.

After the derivatization and subsequent immobilization of TLR-4 (Figure 1a, dashed blue line), the electrochemistry of the surface-bound ferrocene group is seen to be largely unchanged. To ensure that TLR-4 was successfully immobilized, a modified enzyme-linked immunosorbent assay was performed on the TLR-4 modified 30%MUA/5%MFc/65%MUO SAM-based electrode. Based on previous literature,[41] the absorbance at 650 nm (A_{650}) was measured in the solution contacting the coated electrode. When TLR-4 was immobilized on the SAM, the A_{650} value was 0.136, whereas the Au control gave an A_{650} value of only 0.04. This mesaurement demonstrated that TLR-4 was successfully immobilized on the modified SAM.

To confirm that the derivatization of the SAM was performed correctly, both contact angle and X-ray photoelectron spectroscopy (XPS) measurements were performed. The contact angle (Figure S-2) at each stage of sensor construction (Scheme 1) follows the expected trend of increasing hydrophilicity during construction. The contact angle decreases from ca. 80 ° for Au to ca. 35 ° for the SAM and the Ni^{2+}-NTA stages of sensor fabrication. When TLR-4 is attached to the SAM, the contact angle is seen to decrease further to ca. 22 °, as would be expected for a hydrophilic protein.

XPS measurements at the Ni^{2+}-NTA stage of sensor construction showed the expected ratios between the elements on the surface (Figures 2 and S-3, Table S-1). The deconvolution of the C1s spectra resulted in four peaks, representing the sp^2 and sp^3 C-C bonds as well as the C-O single and double bonds. There was strong agreement between the O1s and C1s spectra, with both providing a C-O:C=O ratio of ca. 1.3:1, similar to the predicted value of 1.2:1. The S2p spectra demonstrated both bound and unbound thiols (Figure S-3a), which has been previously seen for electrochemically stable SAMs on Au.[42] The N1s spectra could not be deconvoluted into separate peaks for amines and amides (Figure S-3b), due to their similar binding energies. It was also observed that the binding energy of the Ni present in the SAM (856.6 eV) had shifted from that of the precursor ($NiSO_4$, 857.3 eV) to that of Ni^{2+} interaction with hydroxyl groups (e.g., $Ni(OH)_2$), indicating the successful chelation of Ni^{2+} by the NTA functional groups in the SAM (Figure S-3c).[43]

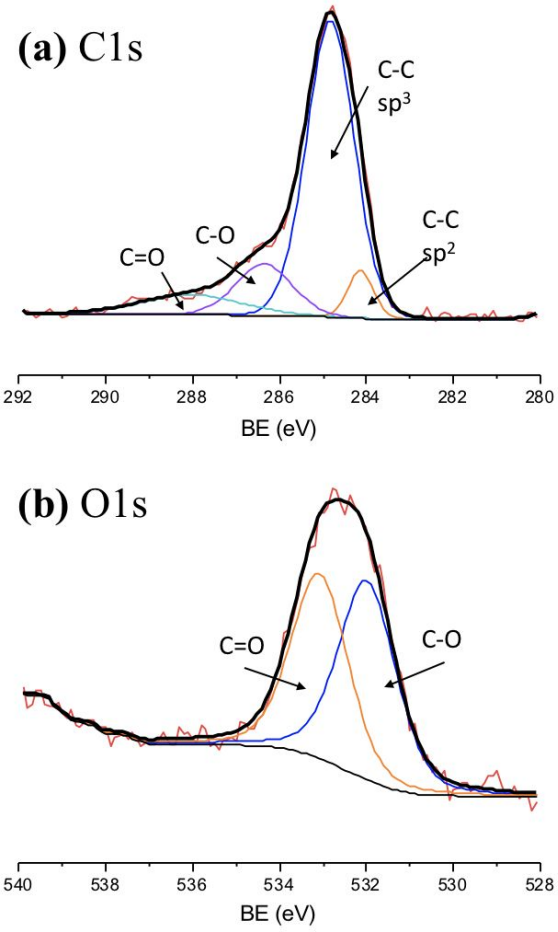

Figure 2. X-ray photoelectron spectra of the **(a)** C1s and **(b)** O1s electrons of a Ni^{2+}-NTA modified 30%MUA/5%MFc/65%MUO SAM on Au.

These results indicate that these SAM modifications, including the attachment of TLR-4 to the outer surface, did not interfere with the underlying monolayer and that the similarity between the CVs in Figure 1a is not due to a failure in the sensor construction. The ferrocene CV is also quite stable, with minimal changes seen over 50 cycles, further supporting the use of this SAM as the foundation of our TLR-4-based sensor. While these data cannot confirm the proposed SAM structure shown in Scheme 1, they do provide confidence that the modification procedures were successful and that TLR-4 was immobilized on the modified SAM surface.

Electrochemistry of TLR-4 Sensor in the Presence of Ferrocyanide

Figure 3a presents voltammograms for a pair of TLR-4-modified sensors exposed to 5 mM $K_4Fe(CN)_6$ in 0.2 M phosphate buffer and subjected to CV analysis. The voltammogram in red corresponds to a sensor prepared without ferrocene in the SAM and shows nearly zero current over the full potential range tested, despite the fact that ferrocyanide ions are present and could be oxidized to ferricyanide at potentials positive of the ferro/ferricyanide formal potential, which is +0.25 V vs Ag/AgCl in this medium. As noted earlier, this oxidation reaction is inhibited because of the large spatial separation between the gold electrode and the ferrocyanide ions, enforced by the SAM.

The voltammogram for the sensor with 5% ferrocene in the SAM is very different, showing a large peak near +0.35 V on the anodic scan and a broad reductive feature at potentials negative of +0.30 V in the cathodic scan. The oxidation peak in this CV is consistent with mediated oxidation of ferrocyanide by the surface-attached ferrocenyl-carboxamide groups, as has been previously described.[22] The mediation reaction is highly favored because the ferrocene redox potential is more positive than the ferrocyanide redox potential, which makes ferricinium a sufficiently potent oxidant to oxidize ferrocyanide. The reverse reaction causing ferricyanide reduction is disfavored, again due to the relative values of the ferrocene and ferrocyanide redox potentials, but it can apparently still occur to a great enough extent to be detected, as indicated by the presence of cathodic current.

A detailed kinetics study of this electrochemical behavior accounting for all of the relevant reaction rates is beyond the scope of this report. For the present purpose of understanding the TLR-4 sensor operation, it is sufficient to recognize that ferrocyanide redox is almost completely inhibited at the SAM-coated electrode without ferrocene, but is permitted at a

nearly identical electrode with 5% ferrocene in the SAM due to the mediation reaction between surface-confined ferrocene groups and ferrocyanide ions in solution.

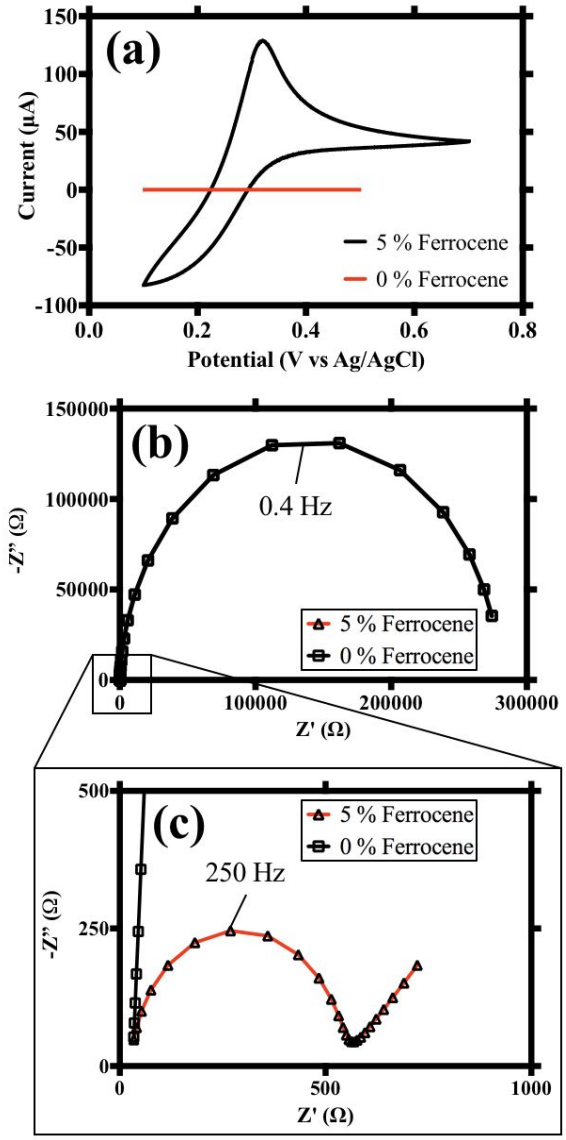

Figure 3. (a) Cyclic voltammograms of TLR-4-modified sensors based on 30%MUA/70%MUO (0% ferrocene) and 30%MUA/5%MFc/65%MUO (5% ferrocene) SAMs on Au. The first complete scan (2nd cycle) is shown for each experiment. **(b-c)** Nyquist plots of TLR-4 modified sensors based on 0% and 5% Ferrocene SAMs. All tests were conducted in 0.2 M pH 7 phosphate buffer + 5 mM $K_4Fe(CN)_6$.

Electrochemical impedance spectroscopy (EIS) analysis was performed on the two electrodes from Figure 3a at an applied potential of +0.3 V. This potential was chosen because it is roughly mid-way between the anodic and cathodic peaks, where the net DC current is near

zero, and because the mediated redox reaction should be sensitive to details of the electrode structure at this potential. Figures 3b and 3c present EIS spectra along with fits to the Randles circuit for both electrodes. Both spectra show semicircles when plotted in complex-plane format but the diameter, which is approximately equal to the R_p value in the Randles equivalent circuit, is much larger for the sensor without ferrocene than for the sensor with ferrocene (ca. 300,000 ohms vs. ca. 600 ohms). This very large difference in resistance is indicative of the redox mediation by the ferrocene groups.

Notably, the time constant (resistance multiplied by capacitance) of the sensor based on a 5% ferrocene SAM is much smaller than that of the analogous 0% ferrocene SAM, which allows for a significantly decreased measurement time. The much lower value for R_p and much shorter time constant in the ferrocene-containing sensor will greatly simplify signal detection, since it produces higher currents and allows for the use of simpler instrumentation.

Response of TLR-4 Sensor to Biological Challenges

To determine the responsiveness of the ferrocene-based TLR-4-modified sensor to the presence of Gram-negative bacteria, TLR-4's canonical target, CV and EIS analyses were performed while challenging the sensor with solutions containing differing amounts of lysed Gram-negative bacteria. Figure 4a demonstrates an increasingly positive CV peak potential and a decreasing peak current as the concentration of lysed Gram-negative bacteria is increased. This is due to the dimerization of TLR-4 at the electrode surface, thus blocking access of solution-based ferrocyanide to the ferrocene active sites in the SAM. As expected, this process of lysed bacteria binding to the TLR-4 sensor has increased the electrochemical irreversibility of the mediation reactions across the SAM, as seen by the positive shift of the anodic peak potential.

Figure 4b also shows a significant increase in the resistance (R_p) with increasing concentration of heat-killed *Salmonella typhimurium* (i.e., lysed). This is again due to dimerization of TLR-4, which blocks access of ferrocyanide to the ferrocenyl-containing SAM. The measured R_p increases by a maximum of ca. 80% over the baseline R_p after the addition of the lysed Gram-negative bacteria following a 20 min incubation period, which is an as-yet unoptimized step in the testing of TLR-based biosensors. The dynamic range of the TLR-4 sensor is excellent (Figure 4b), with a response seen from low concentrations (10^0 lysed cells per mL) to large concentrations (10^5 lysed cells per mL) when the bacteria were introduced to a 10 mL electrochemical cell as lysed cells (to release the lipopolysaccharide from the cellular membranes). This represents a range that easily encompasses the relevant concentrations for human health applications and also demonstrates that the sensitivity of the TLR-4 biosensor was not compromised as compared to previous generations, including the work of Amini *et al*., Lin *et al*. and Yeo *et al*., who also observed a similar logarithmic response over multiple orders of magnitude of target concentrations.[1,7,11,13,15]

The EIS response seen in Figure 4b due to the addition of lysed Gram-negative bacteria is also much larger than the drift of the sensor (ca. 6% per hour, Figure S-4). This provides confidence that the response arises from an interaction between the sensor and the bacterial components, in agreement with published results.[7] It also demonstrates that the TLR-4 modified sensor is stable over the time of measurement in these tests. Similar to our previous work, the addition of Gram-negative bacteria does not result in significant changes to the measured R_p when it is exposed to the electrode at any stage of sensor construction before the incorporation of TLR-4 (Table S-2), especially when compared to the response of the full TLR-4 sensor in the same timeframe.

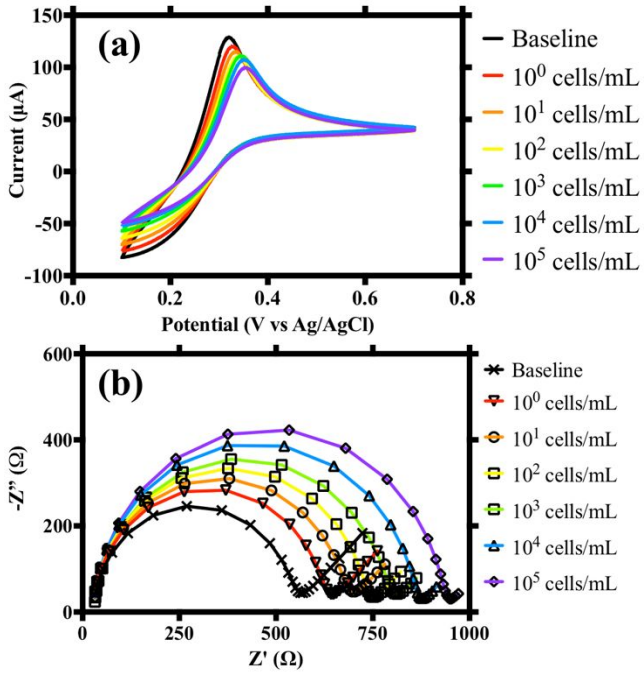

Figure 4. (a) Cyclic voltammograms and **(b)** Nyquist plots of the response of a TLR-4 modified sensor to increasing concentrations of lysed *Salmonella typhimurium* in 0.2 M pH 7 phosphate buffer + 5 mM $K_4Fe(CN)_6$.

To probe the selectivity of the sensor, as well as the possibility that the response is due to non-specific adsorption of bacterial components,[44] the experiment was repeated with both lysed Gram-positive bacterial and viral challenges, with high concentrations (10^4 and 10^5 viral particles or lysed cells per mL) chosen to promote any possible response. As Figures S-5a and S-5b show, both the lysed Gram-positive bacteria *Staphylococcus aureus* (also heat killed) and a UV-inactivated *Rhabdovirus* produced only small perturbations in the measured R_p, with the observed changes being within the range of drift of the sensor (Figure S-4). This provided further confirmation that the response to Gram-negative bacteria in Figure 4a is due to the interactions of TLR-4 and the Gram-negative bacterial components rather than the result of non-specific adsorption. Interestingly, while Amini *et al*. also produced similarly low resistance TLR-4 biosensors through the use of branched dithiols, which typically results in SAMs with less dense packing and greater vulnerability to oxidative desorption by O_2,[45] no control experiments to

assess the drift of the sensor or to determine the specificity towards Gram-positive or viral challenges were performed.[13] Thus, it is difficult to reliably compare our results with theirs.

When a TLR-4 modified sensor is challenged with Gram-negative bacteria in the absence of ferrocyanide, there is no change in the ferrocene voltammograms. This implies that the measured change in R_p likely corresponds to a mass-transfer limited process rather than a change in electron-transfer rates between ferrocene and Au. This insight may be useful in optimizing the sensitivity and performance of future sensors based on the principle of analyte binding coupled to restricted diffusion at an electrochemical sensor surface.

TLR-4 Sensor Response Utilizing a Field-Ready Open-Source Potentiostat

Based on the significantly decreased interfacial resistance with the incorporation of ferrocenyl-terminated thiols into the SAM of the TLR-4 sensor, it was theorized that the response of the sensor could be observed with inexpensive handheld potentiostats as well as the research-grade potentiostats used in the development of electrochemical biosensors. Towards this end, an inexpensive (<$100) open-source potentiostat, based on the work of Rowe *et al*.,[16] was fabricated by a commercial manufacturer and was connected directly to our electrochemical cell (Figure 5a). The potentiostat outputs data via a USB cable connected to a computer running the firmware designed by Rowe *et al*.

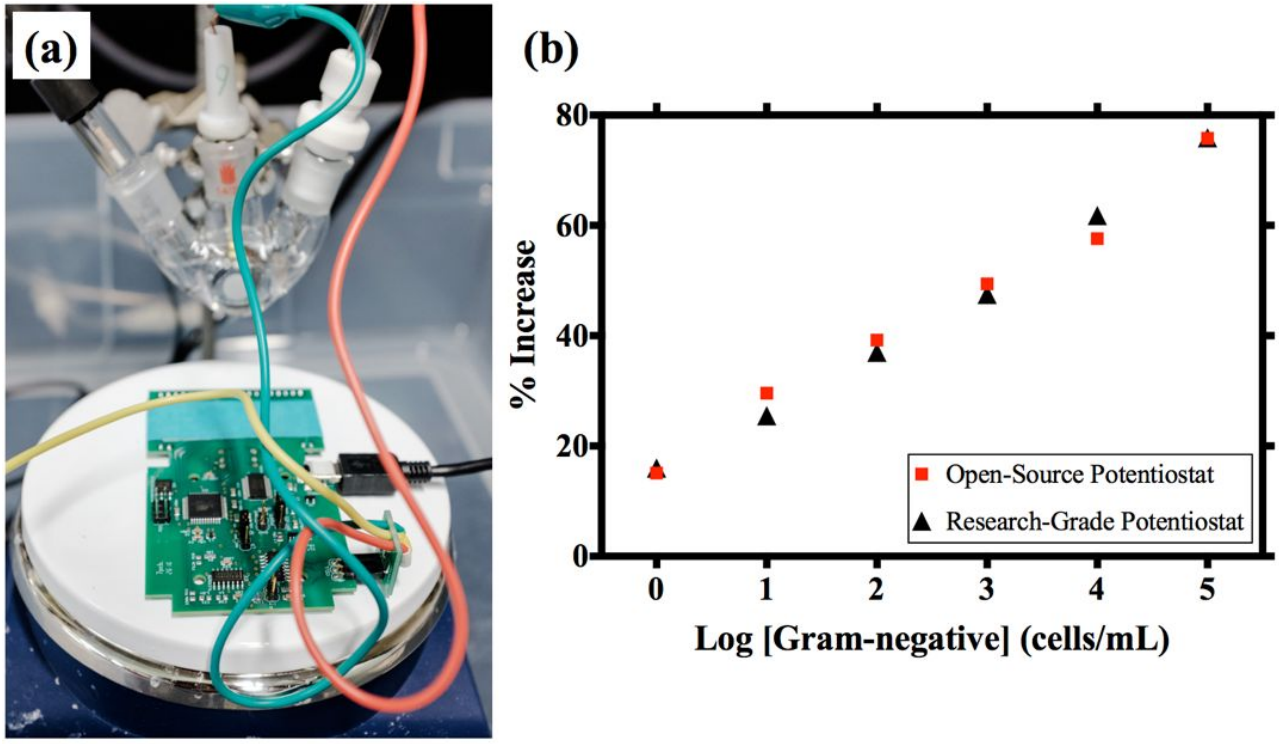

Figure 5. (a) An open-source potentiostat circuit board connected to an electrochemical cell. **(b)** Calculated resistance increase of a TLR-4 modified sensor due to additions of lysed *Salmonella typhimurium*, as measured by both the open-source and research-grade potentiostats in 0.2 M pH 7 phosphate buffer + 5 mM $K_4Fe(CN)_6$.

As the open-source potentiostat cannot perform impedance measurements, polarization resistance measurements with a 10 mV amplitude were performed around the same potential as the impedance performed on the research-grade potentiostat (0.3 V vs Ag/AgCl). This technique, which is common in corrosion research, can rapidly assess the interfacial resistance of an electrode while also employing simpler instrumentation than required for pulsed voltammetry or AC-based electrochemical techniques. This is especially true of the instrumentation required to apply high frequency perturbations, such as during impedance analysis, which is commonly used in comparable TLR biosensor research and in the work described above using the research-grade potentiostat. The application of polarization resistance measurements also provided a rapid measurement time, with each scan requiring only 10 seconds. This is because only one

perturbation frequency (the scan rate) is used, as opposed to the multiple frequencies employed in the case of a typical impedance experiment (10^5-10^{-1} Hz). 10 mV/s was chosen as the equivalent frequency for the LPR tests in this work, as this is a sufficiently slow perturbation such that the measured resistance encompasses the entire impedance arc, as demonstrated in Figure 3c.

Figure 5b shows that there is excellent agreement between the two measurements (resistance vs. baseline signal), with both systems capable of detecting trace amounts of lysed Gram-negative bacteria. As expected, when an analogous test was performed with a TLR-4 modified sensor based on a 0% ferrocene SAM, the open-source potentiostat could not detect a signal due to the very low currents then passed, reinforcing the fact that the ferrocene-mediated oxidation of ferrocyanide is essential for the operation of this system in field-deployable sensors. This represents the first demonstration of a TLR-based biosensor operating on a potentiostat that is amenable to the rapid implementation outside of a laboratory setting.

Summary and Conclusions

In summary, we have successfully designed and constructed a TLR-4 impedance-based bacterial biosensor utilizing ferrocenyl-terminated thiols in a mixed SAM to significantly lower the resistance of the sensor and shorten the measurement time. The sensor fabrication was confirmed with both contact angle measurements and X-ray photoelectron spectroscopy data, as well as a modified immunosorbent assay to demonstrate the TLR-4 immobilization. These sensors were shown to exhibit much higher currents than previously reported TLR biosensors and to respond logarithmically to increasing concentrations of Gram-negative bacteria in solution, while remaining insensitive towards Gram-positive bacteria or viral particles. This

strategy could be readily applied as a diagnostic tool to rapidly differentiate classes of biological agents in many fields as demonstrated with the use of a portable, inexpensive, open-source potentiostat. The interplay of the ferrocene and ferrocyanide electrochemistry could also be taken advantage of with other TLRs to generate a suite of sensors, or through the use of other sensor mechanisms, including antibody-based biosensors.

Acknowledgements

We gratefully acknowledge the Natural Sciences and Engineering Research Council of Canada (NSERC) for the financial support (RGPIN: 2518-2013). The authors also thank the Vanier CGS and Alberta Innovates GSS programs for the support of RMM and NSERC for PDF support of MRY, as well as Dr. Armando Marenco (University of Calgary) for graphical support.

Supporting Information

Supporting Information Available: The following files are available free of charge. Supporting Information Methods and Figues. Equivalent circuit diagram, XPS data, contact angle results, impedance spectra, materials used and additional experimental methods.

References

(1) Bloos, F. Clinical Diagnosis of Sepsis and the Combined Use of Biomarkers and Culture- and Non-Culture-Based Assays. In *Sepsis: Diagnostic Methods and Protocols*; Mancini, N., Ed.; 2015; pp 247–260.

(2) Zaas, a. K.; Burke, T.; Chen, M.; McClain, M.; Nicholson, B.; Veldman, T.; Tsalik, E. L.; Fowler, V.; Rivers, E. P.; Otero, R.; et al. A Host-Based RT-PCR Gene Expression Signature to Identify Acute Respiratory Viral Infection. *Sci. Transl. Med.* **2013**, *5* (203), 203ra126.

(3) Yamanaka, K.; Saito, M.; Kondoh, K.; Hossain, M. M.; Koketsu, R.; Sasaki, T.; Nagatani, N.; Ikuta, K.; Tamiya, E. Rapid Detection for Primary Screening of Influenza A Virus: Microfluidic RT-PCR Chip and Electrochemical DNA Sensor. *Analyst* **2011**, *136* (10), 2064–2068.

(4) Creagh, E. M.; O'Neill, L. A. J. TLRs, NLRs and RLRs: A Trinity of Pathogen Sensors That Co-Operate in Innate Immunity. *Trends Immunol.* **2006**, *27* (8), 352–357.
(5) Park, B. S.; Song, D. H.; Kim, H. M.; Choi, B.-S.; Lee, H.; Lee, J.-O. The Structural Basis of Lipopolysaccharide Recognition by the TLR4-MD-2 Complex. *Nature* **2009**, *458* (7242), 1191–1195.
(6) Kneifel, W.; Leonhardt, W. Testing of Different Antibiotics against Gram-Positive and Gram-Negative Bacteria Isolated from Plant Tissue Culture. *Plant Cell. Tissue Organ Cult.* **1992**, *29*, 139–144.
(7) Mayall, R. M.; Renaud-Young, M.; Chan, N. W. C.; Birss, V. I. An Electrochemical Lipopolysaccharide Sensor Based on an Immobilized Toll-Like Receptor-4. *Biosens. Bioelectron.* **2017**, *87*, 794–801.
(8) Amini, K.; Chan, N. W. C.; Kraatz, H.-B. Toll-like Receptor 3 Modified Au Electrodes: An Investigation into the Interaction of TLR3 Immobilized on Au Surfaces with Poly(I:C). *Anal. Methods* **2014**, *6*, 3322–3328.
(9) She, Z.; Topping, K.; Shamsi, M. H.; Wang, N.; Chan, N. W. C.; Kraatz, H.-B. Investigation of the Utility of Complementary Electrochemical Detection Techniques to Examine the in Vitro Affinity of Bacterial Flagellins for a Toll-like Receptor 5 Biosensor. *Anal. Chem.* **2015**, *87*, 4218–4224.
(10) Amini, K.; Kraatz, H.-B. Toll-like Receptors for Pathogen Detection in Water: Challenges and Benefits. *Int. J. Environ. Anal. Chem.* **2016**, *96* (9), 836–844.
(11) Yeo, T. Y.; Choi, J. S.; Lee, B. K.; Kim, B. S.; Yoon, H. I.; Lee, H. Y.; Cho, Y. W. Electrochemical Endotoxin Sensors Based on TLR4/MD-2 Complexes Immobilized on Gold Electrodes. *Biosens. Bioelectron.* **2011**, *28* (1), 139–145.
(12) Shin, H. J.; Lee, H.; Park, J. D.; Hyun, H. C.; Sohn, H. O.; Lee, D. W.; Kim, Y. S. Kinetics of Binding of LPS to Recombinant CD14, TLR4, and MD-2 Proteins. *Mol. Cells* **2007**, *24* (1), 119–124.
(13) Amini, K.; Ebralidze, I.; Chan, N. W. C.; Kraatz, H.-B. Characterization of TLR4/MD-2-Modified Au Sensor Surfaces. Towards the Detection of Molecular Signatures of Bacteria. *Anal. Methods* **2016**, *8*, 7623–7631.
(14) She, Z.; Topping, K.; Dong, B.; Shamsi, M. H.; Kraatz, H.-B. An Unexpected Use of Ferrocene. A Scanning Electrochemical Microscopy Study of a Toll-like Receptor Array and Its Interaction with E. Coli. *Chem. Commun.* **2017**, *53*, 2946–2949.
(15) Lin, D.; Harris, K. D.; Chan, N. W. C.; Jemere, A. B. Nanostructured Indium Tin Oxide Electrodes Immobilized with Toll-like Receptor Proteins for Label-Free Electrochemical Detection of Pathogen Markers. *Sensors Actuators, B Chem.* **2018**, *257*, 324–330.
(16) Rowe, A. a.; Bonham, A. J.; White, R. J.; Zimmer, M. P.; Yadgar, R. J.; Hobza, T. M.; Honea, J. W.; Ben-Yaacov, I.; Plaxco, K. W. Cheapstat: An Open-Source, "Do-It-Yourself" Potentiostat for Analytical and Educational Applications. *PLoS One* **2011**, *6* (9), e23783.
(17) Rowe, G. K.; Creager, S. E. Redox and Ion-Pairing Thermodynamics in Self -Assembled Monolayers. *Langmuir* **1991**, *7*, 2307–2312.
(18) Creager, S. E.; Hockett, L. A.; Rowe, G. K. Consequence of Microscopic Surface Roughness for Molecular Self-Assembly. *Langmuir* **1992**, *8* (12), 854–861.
(19) Ulman, a. Formation and Structure of Self-Assembled Monolayers. *Chem. Rev.* **1996**, *96* (4), 1533–1554.
(20) Love, J. C.; Estroff, L. A.; Kriebel, J. K.; Nuzzo, R. G.; Whitesides, G. M. Self-

Assembled Monolayers of Thiolates on Metals as a Form of Nanotechnology. *Chem. Rev.* **2005**, *105* (4), 1103–1169.

(21) Rickert, J.; Göpel, W.; Beck, W.; Jung, G.; Heiduschka, P. A "mixed" Self-Assembled Monolayer for an Impedimetric Immunosensor. *Biosens. Bioelectron.* **1996**, *11* (8), 757–768.

(22) Alleman, K. S.; Weber, K.; Creager, S. E. Electrochemical Rectification at a Monolayer-Modified Electrode. *J. Phys. Chem.* **1996**, *100* (42), 17050–17058.

(23) Sumner, J. J.; Weber, K. S.; Hockett, L. a; Creager, S. E. Long-Range Heterogeneous Electron Transfer between Ferrocene and Gold Mediated by n-Alkane and N-Alkyl-Carboxamide Bridges. *J. Phys. Chem. B* **2000**, *104*, 7449–7454.

(24) Civic, M. R.; Dinolfo, P. H. Electrochemical Rectification of Redox Mediators Using Porphyrin-Based Molecular Multilayered Films on ITO Electrodes. *ACS Appl. Mater. Interfaces* **2016**, *8*, 20465–20473.

(25) Feng, L.; Sivanesan, A.; Lyu, Z.; Offenhäusser, A.; Mayer, D. Electrochemical Current Rectification-a Novel Signal Amplification Strategy for Highly Sensitive and Selective Aptamer-Based Biosensor. *Biosens. Bioelectron.* **2015**, *66*, 62–68.

(26) Aoki, H.; Tao, H. Signal Enhancement for Gene Detection Based on a Redox Reaction of [Fe(CN)(6)](4-) Mediated by Ferrocene at the Terminal of a Peptide Nucleic Acid as a Probe with Hybridization-Amenable Conformational Flexibility. *Anal. Sci.* **2008**, *24* (7), 929–933.

(27) Azzaroni, O.; Mir, M.; Álvarez, M.; Tiefenauer, L.; Knoll, W. Electrochemical Rectification by Redox-Labeled Bioconjugates: Molecular Building Blocks for the Construction of Biodiodes. *Langmuir* **2008**, *24*, 2878–2883.

(28) Feng, L.; Lyu, Z.; Offenhäusser, A.; Mayer, D. Multi-Level Logic Gate Operation Based on Amplified Aptasensor Performance. *Angew. Chemie - Int. Ed.* **2015**, *54* (26), 7693–7697.

(29) Imabayashi, S.; Iida, M.; Hobara, D.; Feng, Z. Q.; Niki, K.; Kakiuchi, T. Reductive Desorption of Carboxylic-Acid-Terminated Alkanethiol Monolayers from Au(111) Surfaces. *J. Electroanal. Chem.* **1997**, *428*, 33–38.

(30) Arnold, R.; Azzam, W.; Terfort, A.; Wöll, C. Preparation, Modification, and Crystallinity of Aliphatic and Aromatic Carboxylic Acid Terminated Self-Assembled Monolayers. *Langmuir* **2002**, *18*, 3980–3992.

(31) Beulen, M. W. J.; Veggel, F. C. J. M. Van; Reinhoudt, D. N. Coupling of Acid – Base and Redox Functions in Mixed Sulfide Monolayers on Gold. *Chem. Commun.* **1999**, 503–504.

(32) Rowe, G. K.; Creager, S. E. Chain Length and Solvent Effects on Competitive Self-Assembly of Ferrocenylhexanethiol and 1 -Alkanethiols onto Gold. *Langmuir* **1994**, *10*, 1186–1192.

(33) Auletta, T.; Van Veggel, F. C. J. M.; Reinhoudt, D. N. Self-Assembled Monolayers on Gold of Ferrocene-Terminated Thiols and Hydroxyalkanethiols. *Langmuir* **2002**, *18*, 1288–1293.

(34) Le, T. T.; Wilde, C. P.; Grossman, N.; Cass, A. E. G. A Simple Method for Controlled Immobilization of Proteins on Modified SAMs. *Phys. Chem. Chem. Phys.* **2011**, *13*, 5271–5278.

(35) Folkers, J. P.; Laibinis, P. E.; Whitesides, G. M. Self-Assembled Monolayers of Alkanethiols on Gold: The Adsorption and Wetting Properties of Monolayers Derived from Two Components with Alkane Chains of Different Lengths. *J. Adhes. Sci. Technol.*

1992, *6* (12), 1397–1410.
(36) Liu, G.; Böcking, T.; Gooding, J. J. Diazonium Salts: Stable Monolayers on Gold Electrodes for Sensing Applications. *J. Electroanal. Chem.* **2007**, *600* (2), 335–344.
(37) Gooding, J. J. Advances in Interfacial Design for Electrochemical Biosensors and Sensors: Aryl Diazonium Salts for Modifying Carbon and Metal Electrodes. *Electroanalysis* **2008**, *20* (6), 573–582.
(38) Chapman, R. G.; Ostuni, E.; Yan, L.; Whitesides, G. M. Preparation of Mixed Self-Assembled Monolayers (SAMs) That Resist Adsorption of Proteins Using the Reaction of Amines with a SAM That Presents Interchain Carboxylic Anhydride Groups. *Langmuir* **2000**, *16*, 6927–6936.
(39) Weber, K.; Hockett, L.; Creager, S. Long-Range Electronic Coupling between Ferrocene and Gold in Alkanethiolate-Based Monolayers on Electrodes. *J. Phys. Chem. B* **1997**, *101* (41), 8286–8291.
(40) Lukaszewski, M.; Soszko, M.; Czerwinski, A. Electrochemical Methods of Real Surface Area Determination of Noble Metal Electrodes - an Overview. *Int. J. Electrochem. Sci.* **2016**, *11* (6), 4442–4469.
(41) Bhimji, A.; Zaragoza, A.; Live, L.; Kelley, S. Electrochemical Enzyme-Linked Immunosorbent Assay Featuring Proximal Reagent Generation: Detection of Human Immunodeficiency Virus Antibodies in Clinical. *Anal. Chem.* **2013**, *84* (14), 6813–6819.
(42) Techane, S. D.; Gamble, L. J.; Castner, D. G. X-Ray Photoelectron Spectroscopy Characterization of Gold Nanoparticles Functionalized with Amine-Terminated Alkanethiols. *Biointerphases* **2011**, *6* (3), 98–104.
(43) Du Roure, O.; Debiemme-Chouvy, C.; Malthête, J.; Silberzan, P. Functionalizing Surfaces with Nickel Ions for the Grafting of Proteins. *Langmuir* **2003**, *19*, 4138–4143.
(44) Zhou, M.; Liu, H.; Venkiteshwaran, A.; Kilduff, J.; Anderson, D. G.; Langer, R.; Belfort, G. High Throughput Discovery of New Fouling-Resistant Surfaces. *J. Mater. Chem.* **2011**, *21*, 693–704.
(45) Hou, W.; Dasog, M.; Scott, R. W. J. Probing the Relative Stability of Thiolate- and Dithiolate-Protected Au Monolayer-Protected Clusters. *Langmuir* **2009**, *25* (22), 12954–12961.